

Can we explain AMS-02 antiproton and positron excesses simultaneously by nearby supernovae without pulsars nor dark matter?

Kazunori Kohri^{1,*}, Kunihiro Ioka¹ Yutaka Fujita², and Ryo Yamazaki^{3,4}

¹*Theory Center, IPNS, KEK, and Sokendai, 1-1 Oho, Tsukuba 305-0801, Japan*

²*Department of Earth and Space Science, Graduate School of Science, Osaka University, Toyonaka, Osaka 560-0043, Japan*

³*Department of Physics and Mathematics, Aoyama-Gakuin University, Kanagawa 252-5258, Japan*

⁴*Harvard-Smithsonian Center for Astrophysics, MS-51, 60 Garden Street, Cambridge, MA 02138, USA*

*E-mail: kohri@post.kek.jp

.....
We explain the excess of the antiproton fraction recently reported by the AMS-02 experiment by considering collisions between cosmic-ray protons accelerated by a local supernova remnant (SNR) and the surrounding dense cloud. The same “ pp collisions” provide the right ratio of daughter particles to fit the observed positron excess simultaneously in the natural model parameters. The supernova happened in relatively lower metallicity than the major cosmic-ray sources. The cutoff energy of electrons marks the supernova age of $\sim 10^5$ years, while the antiproton excess may extend to higher energy. Both antiproton and positron fluxes are completely consistent with our predictions in Ref. [4].

1. Introduction

Recently the Alpha Magnetic Spectrometer (AMS-02) on the International Space Station has reported that the antiproton to proton ratio stays constant from 20 GeV to 450 GeV kinetic energy [1]. This behavior cannot be explained by the secondary antiprotons from collisions of ordinary cosmic rays with interstellar medium [e.g., 2]. This suggests a new source such as astrophysical accelerators and annihilating or decaying dark matter, although there are still uncertainties in the background modeling [3].

The excess of antiprotons looks surprisingly similar to what we predicted [4] when the PAMELA experiment detected the positron excess [5] and the Fermi, HESS, and ATIC/PPB-BETS experiments observed the electron anomaly [6–8]. We considered recent supernova explosions in a dense gas cloud (DC) near the Earth. The antiprotons and positrons are produced as secondaries by the pp collisions between cosmic-ray protons accelerated by the supernova remnant (SNR) and target protons in a DC which surrounds the SNRs [4]. Since the fundamental process determines the branching fraction, the positron excess should accompany the antiproton excess.

There are several variants of such a hadronic model, e.g., the reacceleration of secondaries by SNR shocks [9] or the non-standard propagation that increases secondaries from ordinary cosmic-ray collisions with interstellar matter [10–12]. Since the element ratio is the same as the ordinary cosmic rays in these models, the ratio of secondaries (e.g., Li, Be, B) to primaries

(C, N, O) must also rise with energy beyond ~ 100 GeV, which is not observed yet [13–15]. In contrast to these models, our model can accommodate the observations as shown below.

Before AMS-02, the antiproton observations were consistent with the secondary background [16]. Thus the leading models for the positron excess are leptonic, such as pulsars and leptophilic dark matter [e.g., 17–20]. The pulsars cannot usually explain the antiproton excess. On the other hand, the dark matter for the positron excess is now severely constrained by other messengers such as gamma-rays and cosmic microwave background [e.g., 21, 22], and hence we may need fine tunings in dark matter models to reproduce both the antiproton and positron excesses [3, 23–25].

Following Occam’s razor, we reexamine our nearby SNR model and simultaneously fit the antiproton fraction, positron fraction, and total electron and positron flux in light of new AMS-02 data. In particular the pp collisions give the correct branching fraction for the observed positron to antiproton ratio. Throughout this paper we adopt units of $c = \hbar = k_B = 1$.

2. Supernova explosions in a Dense Cloud

Here we consider supernova explosions which occurred around $\sim 10^5 - 10^6$ years ago in a DC. We assume the DC is located at around ~ 100 – 200 pc away from the Earth like the progenitor DCs that produced the Local Bubble (LB) or Loop I. In general a massive star tends to be born in a giant DC [26] which explodes as a supernova. In this paper, we assume that the Giant DC is ionized and the temperature is approximately $\sim 10^4$ K at the time of its explosion [27]. The shock of an SNR accelerates protons, which produce copious energetic mesons (pions and kaons, etc.) and baryons (antiproton, proton, antineutron, neutron, etc.) through the pp collisions in the surrounding DC. The mesons further decay into energetic positrons, electrons, gamma-rays, and neutrinos. In total those local secondary particles can be observed at the Earth as cosmic-rays in addition to the standard background components.

The energy spectrum of the accelerated protons is parametrized by

$$\frac{dn_p}{dE_p} \propto E_p^{-s} e^{-\frac{E_p}{E_{\max,p}}}, \quad (1)$$

where s is the spectral index. The age of SNR, t_{age} , approximately determines the maximum energy [28],

$$E_{\max,p} \sim 2 \times 10^2 v_{s,8}^2 \left(\frac{B_d}{10 \mu\text{G}} \right) \left(\frac{t_{\text{age}}}{10^5 \text{yr}} \right) \text{ TeV}, \quad (2)$$

where the shock velocity, v_s , is $v_{s,8} = v_s / 10^8 \text{ cm s}^{-1} \sim O(1)$. B_d is the downstream magnetic field. We take the minimum energy of the protons to be its rest mass. We assume that the supernova explodes at the center of a DC for simplicity. In addition, we also assume that the acceleration stops when the Mach number of the shock decreases to 7 [4]. We define this time as the acceleration time $t_{\text{acc}} = t_{\text{age}}$, and the energy spectrum at this time is given by $s \sim 2$ and $E_{\max,p} \sim 120$ TeV [4]. The SNR continues to expand even at $t_{\text{age}} > t_{\text{acc}}$.

The radius is 50 pc at $t_{\text{age}} = 5 \times 10^5$ yr. Since it is comparable to the size of a giant DC, R_{DC} , [29] and the initial energy of the ejecta from the supernovae is larger than the binding energy of a DC, the cloud would be destroyed around this time. Until it is destroyed, the DC is illuminated by the accelerated protons from the inside with the spectrum of Eq. (1) given at $t_{\text{age}} \sim t_{\text{acc}}$. The duration of the exposure, t_{pp} , could be approximated by the time elapsing

from the explosion of the supernovae to the destruction of the DC because the timescale t_{acc} is shorter than 5×10^5 yr.

After the destruction of the DC, the produced charged particles such as \bar{p} , p , e^+ , or e^- propagate through diffusion processes and reach to the Earth. Since we assume that the DC has already been destroyed well before the present epoch, there are some differences in arrival times between those charged particles and massless neutral particles such as photons. It should be a reasonable assumption that we would not detect any photon and neutrino signals from the DC $\sim 10^{5-6}$ years after the destruction of the DC.

We have calculated spectra of those daughter particles through the pp collisions by performing the PYTHIA Monte-Carlo event generator [30] (See [28] for the details). Then we solve the diffusion equation of the charged particle “ i ” (i runs \bar{p} , p , e^+ , and e^-),

$$\frac{\partial f_i}{\partial t} = K(\varepsilon_i) \Delta f_i + \frac{\partial}{\partial \varepsilon_i} [B(\varepsilon_i) f_i] + Q(\varepsilon_i) \quad (3)$$

where $f_i(t, x, \varepsilon_i)$ is the distribution function of an i particle, and $\varepsilon_i = E_i/\text{GeV}$ with E_i being the energy of the i particle. The flux is given by

$$\Phi_i(t, x, \varepsilon_i) = \frac{1}{4\pi} f_i. \quad (4)$$

We adopt a diffusion model 08-005 given in [31] with the diffusion coefficient,

$$K(\varepsilon_e) = K_0 \left(1 + \frac{\varepsilon_e}{3\text{GeV}}\right)^\delta, \quad (5)$$

with $K_0 = 2 \times 10^{28} \text{cm}^2 \text{s}^{-1}$ and $\delta = 0.42$ [24, 32, 33]. The cooling rate through the synchrotron emission and the inverse Compton scattering is collectively parametrized to be [34]

$$B(\varepsilon_e) \sim 10^{-16} \text{s}^{-1} \varepsilon_e^2 \left[0.2 \left(\frac{B_{\text{diff}}}{3\mu\text{G}} \right)^2 + 0.9 \right], \quad (6)$$

where B_{diff} is the magnetic field outside the DC. This set of the parameters approximately corresponds to the MED model of the cosmic-ray propagation [35].

If we assume that the timescale of the production is shorter than that of the diffusion, $\sim d^2/(Kc)$ with d being the distance to the source, and the source of the daughter particles is spatially localized sufficiently, we can use the known analytical solution in [36]. When the shape of the source spectrum is a power-law with an index α to be

$$Q = Q_0 \varepsilon^{-\alpha} \delta(x) \delta(t), \quad (7)$$

then the solution is given by

$$f_e = \frac{Q_0}{\pi^{3/2} d_{\text{diff}}^3} \varepsilon_e^{-\alpha} \left(1 - \frac{\varepsilon_e}{\varepsilon_{\text{cut}}}\right)^{\alpha-2} e^{-\left(\frac{\bar{d}}{d_{\text{diff}}}\right)^2}, \quad (8)$$

where $\varepsilon_{\text{cut}} = \varepsilon_e^2/Bt_{\text{diff}}$, and the diffusion length is represented by

$$d_{\text{diff}} = 2\sqrt{Kt_{\text{diff}} \frac{1 - (1 - \frac{\varepsilon_e}{\varepsilon_{\text{cut}}})^{1-\delta}}{(1-\delta)\frac{\varepsilon_e}{\varepsilon_{\text{cut}}}}}. \quad (9)$$

\bar{d} means the effective distance to the source by spatially averaging the distance to the volume element of the source, and we assume $\alpha \simeq s$. We approximately have

$$Q_0 \varepsilon_i^{-\alpha} \sim V_s t_{pp} \frac{d^2 n_i}{dt dE_i} \quad (10)$$

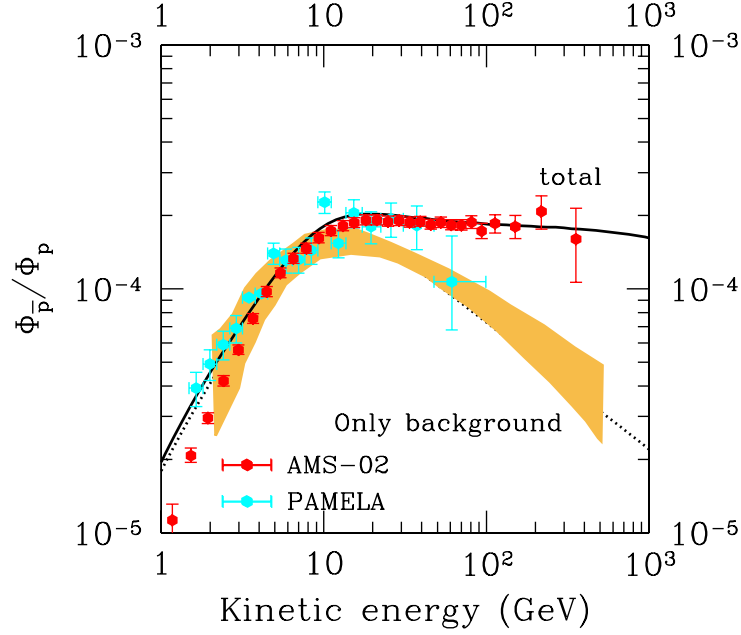


Fig. 1 Antiproton fraction fitted to the data. The data points are taken from [1] for AMS-02, and from [16] for PAMELA. The dotted line is plotted only by using the background flux [37]. The shadow region represents the uncertainties of the background flux among the propagation models shown in [1]. Cosmic rays below an energy $\lesssim 10\text{GeV}$ are affected by the solar modulation. We choose the background line and its uncertainty band only for a demonstration purpose. This choice is not essential for our conclusion (See the text about Fig. 3).

with V_s the source volume where

$$\frac{d^2 n_i}{dt dE_i} = \int dE_p n_0 \frac{dn_p}{dE_p} \sum_j g_j \frac{v_p d\sigma_j}{dE_i}. \quad (11)$$

The differential cross section of the “ j ”-mode for the production of the i particle is represented to be $d\sigma_j(E_p, E_i)/dE_i$ with the multiplicity into the j -mode, $g_j = g_j(E_p, E_i)$. $v_p = v_p(E_p)$ is the velocity of the primary proton. We also consider the free neutron (antineutron) decay for the electron (positron) production process, which is not included in the original version of PYTHIA. The initial proton spectrum $\frac{dn_p}{dE_p}$ can be obtained by a normalization to satisfy

$$V_s \int dE_p \frac{dn_p}{dE_p} = E_{\text{tot,p}}. \quad (12)$$

For the local propagation of protons and antiprotons, their cooling is negligible unlike electrons and positrons. Additionally we can omit annihilations of antiprotons through scattering off the background protons because the scattering rate is small. We can also omit convection by interstellar turbulence within the galaxy. An analytical solution for the proton and the antiproton is also given by the same equation as Eq. (8) with a limit of $\varepsilon_p/\varepsilon_{\text{cut}} = 0$.

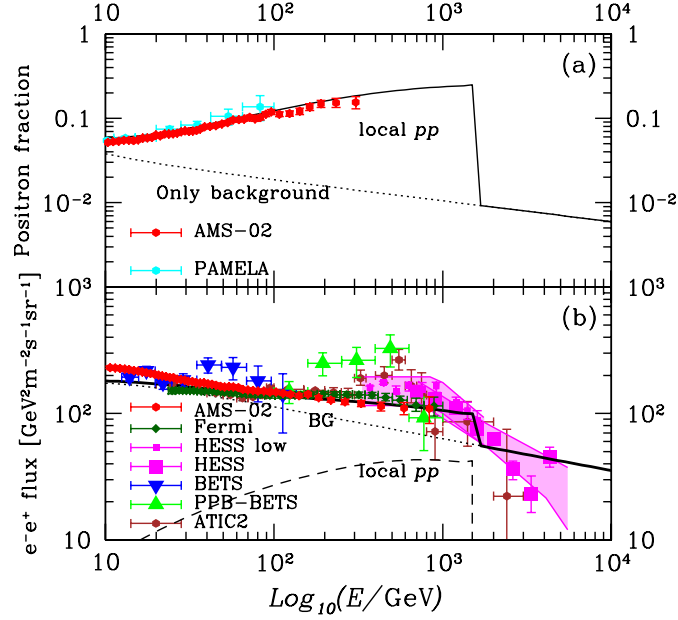


Fig. 2 (a) Positron fraction (solid line), which includes the electrons and positrons coming from the DC and background electrons (dotted line, for example see Refs. [31, 34]). Filled circles correspond to the AMS-02 data [1, 38, 39] and PAMELA data [5] (b) Total electron and positron flux (solid line). The flux of the electrons and positrons created only in the DC (background) is plotted by the dashed (dotted) line. Observational data by AMS-02, Fermi, HESS, BETS, PPB-BETS, and ATIC2 [6–8, 40] are also plotted. The shadow region represents the uncertainty of the HESS data.

3. Antiproton and positron fittings

In Fig. 1, we plot the antiproton fraction at the Earth in our model (See also a similar model named “model B” given in Ref. [4]). For the background flux, we adopted the 20% smaller value of the mean value shown in [37]. Here, the radius of a spherical DC, $R_{\text{DC}} = 40$ pc is adopted. The target proton density is set to be $n_0 = 50 \text{ cm}^{-3}$. The spectral index $s = 2.15$ and the maximum energy, $E_{\text{max}} = 100$ TeV, are assumed. We take the duration of the pp collision to be $t_{pp} = 2 \times 10^5$ yr. The total energy of the accelerated protons is assumed to be $E_{\text{tot,p}} = 2.6 \times 10^{50}$ erg. The distance to the front of the DC is set to be $d = 200$ pc. About the diffusion time of e^- and e^+ , $t_{\text{diff}} = 2 \times 10^5$ yr is adopted. We take the magnetic field outside the DC to be $B_{\text{diff}} = 3 \mu\text{G}$ (See [4] for the further details).

In Fig. 2, we also plot the positron fraction and the total $e^- + e^+$ flux. It is remarkable that we can automatically fit the observational data of both the positron fraction and the total $e^- + e^+$ flux by using the same set of the parameters [4]. Here the cooling cutoff energy is approximately given by $\varepsilon_{\text{cut}} = \epsilon_e^2 / B t_{\text{diff}} \sim 1 \text{ TeV} (t_{\text{diff}} / 2 \times 10^5 \text{ yrs})^{-1}$.

The positron fraction rises at higher energies than that of the antiproton fraction (Fig. 3), because the spectral index of the background antiproton is harder than that of the background positron. This comes from a difference between their cooling processes. Only for background positrons and electrons the cooling is effective in the current situation.

In Fig. 3, we plot the positron to antiproton ratio as a function of the rigidity. Here the local components represent the contribution of the nearby SNRs produced only by the pp collisions. From this figure, we find that both of the positron and the antiproton can be consistently fitted only by adding astrophysical local contributions produced from the same pp collision sources.

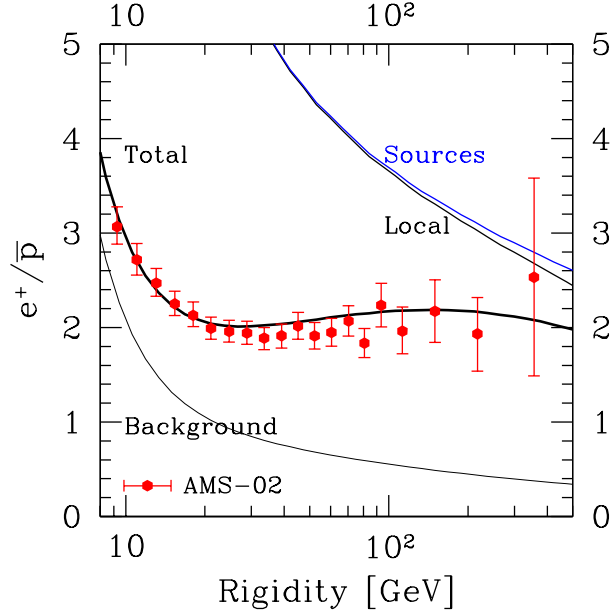


Fig. 3 Positron to antiproton ratio as a function of the rigidity with adding the local components produced by the pp collisions occurred at SNRs near the Earth. The thick solid line represents the case of the total flux. From the upper right to the lower left, we plot the flux ratios of 1) the one at the source (without cooling), 2) only the local components, 3) the total of the local and the background components, and 4) only the background components. The observational data reported by AMS-02 are also plotted.

4. Conclusion

We have discussed the anomaly of the antiproton fraction recently-reported by the AMS-02 experiment. By considering the same origin of the pp collisions between cosmic-ray protons accelerated by SNRs and a dense cloud which surrounds the SNRs, we can fit the data of the observed antiproton and positron simultaneously in the natural model parameters. The observed fluxes of both antiprotons and positrons are consistent with our predictions shown in Ref. [4].

Regardless of the model details, the ratio of antiproton to positron is essentially determined by the fundamental branching fraction into each mode of the pp collisions. Thus the observed antiproton excess should entail the positron excess, and vice versa. This does not depend on the propagation model since both antiparticles propagate in a similar way below the cooling cutoff energy \sim TeV.

The cutoff energy of e^- cooling marks the supernova age of $\sim 10^5$ years [19, 41], while we also expect a e^+ cutoff. The trans-TeV energy will be probed by the future CALET, DAMPE and CTA experiments [42, 45]. An anisotropy of the arrival direction is also a unique signature, e.g., [43]. We may estimate the amplitude of anisotropy as $\delta_e \sim 3d/2ct_{\text{diff}} \sim 0.5\%$, which is below the upper limits by Fermi observations [44].

The boron to carbon ratio as well as the Li to carbon ratio have no clear excesses [1]. This suggests that the carbon fraction of the excess-making cosmic rays is smaller than that of the ordinary cosmic rays. In general the supernovae in the DC would not be the main channel of cosmic-ray production. Most of cosmic rays above ~ 30 GeV may be produced in chemically enriched regions, such as superbubbles, as implied by the hard spectrum of cosmic-ray helium [46]. Or the carbon abundance of the destroyed DC might happen to be lower than the Galactic average [4].

We should be careful about the background systematics. In particular the propagation uncertainties yield the largest errors [3, 47]. However, in the energy region above ~ 100 GeV where the background contribution is small, the observed positron to antiproton ratio is very close to the branching fraction of the pp collisions (source components in Fig. 3). This fact is free from the background choice and partially supports our model.

ACKNOWLEDGMENTS

This work was supported in part by Grant-in-Aid for Scientific research from the Ministry of Education, Science, Sports, and Culture (MEXT), Japan, Nos. 26105520, 15H05889 (K.K.), 26247042 (K.K. and K.I.), 26287051, 24103006, 24000004 (K.I.), 15K05080 (Y.F.), and 15K05088 (R.Y.). The work of K.K. and K.I. was also supported by the Center for the Promotion of Integrated Science (CPIS) of Sokendai (1HB5804100).

Note added

While finalizing this manuscript, Ref. [48] appeared which has some overlaps with this work.

References

- [1] AMS-02 Collaboration, “AMS Days at CERN” and Latest Results, 15, April, 2015.
- [2] M. Kachelriess, I. V. Moskalenko and S. S. Ostapchenko, *Astrophys. J.* **803**, no. 2, 54 (2015) [arXiv:1502.04158 [astro-ph.HE]].
- [3] G. Giesen, M. Boudaud, Y. Genolini, V. Poulin, M. Cirelli, P. Salati, P. D. Serpico and J. Feng *et al.*, arXiv:1504.04276 [astro-ph.HE].
- [4] Y. Fujita, K. Kohri, R. Yamazaki and K. Ioka, *Phys. Rev. D* **80**, 063003 (2009) [arXiv:0903.5298 [astro-ph.HE]].
- [5] O. Adriani *et al.* [PAMELA Collaboration], *Nature* **458**, 607 (2009) [arXiv:0810.4995 [astro-ph]].
- [6] J. Chang, *et al.*, *Nature* **456**, 362 (2008); S. Torii, *et al.*, arXiv:0809.0760.
- [7] A. A. Abdo *et al.* [The Fermi LAT Collaboration], arXiv:0905.0025 [astro-ph.HE].
- [8] F. Aharonian, *et al.*, *Phys. Rev. Lett.* **101**, 261104 (2008), arXiv:0905.0105 [astro-ph.HE].
- [9] P. Blasi and P. D. Serpico, *Phys. Rev. Lett.* **103**, 081103 (2009) [arXiv:0904.0871 [astro-ph.HE]].
- [10] K. Blum, B. Katz and E. Waxman, *Phys. Rev. Lett.* **111**, no. 21, 211101 (2013) [arXiv:1305.1324 [astro-ph.HE]].
- [11] R. Cowsik, B. Burch and T. Madziwa-Nussinov, *Astrophys. J.* **786**, 124 (2014) [arXiv:1305.1242 [astro-ph.HE]].
- [12] Y. Q. Guo, H. B. Hu and Z. Tian, arXiv:1412.8590 [astro-ph.HE].
- [13] P. Mertsch and S. Sarkar, *Phys. Rev. Lett.* **103**, 081104 (2009) [arXiv:0905.3152 [astro-ph.HE]].
- [14] I. Cholis and D. Hooper, *Phys. Rev. D* **89**, no. 4, 043013 (2014) [arXiv:1312.2952 [astro-ph.HE]].
- [15] P. Mertsch and S. Sarkar, *Phys. Rev. D* **90**, 061301 (2014) [arXiv:1402.0855 [astro-ph.HE]].
- [16] O. Adriani *et al.*, *Phys. Rev. Lett.* **102**, 051101 (2009).
- [17] P. D. Serpico, *Astropart. Phys.* **39-40**, 2 (2012) [arXiv:1108.4827 [astro-ph.HE]].

-
- [18] Y. Z. Fan, B. Zhang and J. Chang, *Int. J. Mod. Phys. D* **19**, 2011 (2010) [arXiv:1008.4646 [astro-ph.HE]].
 - [19] K. Ioka, *Prog. Theor. Phys.* **123**, 743 (2010) [arXiv:0812.4851 [astro-ph]].
 - [20] K. Kashiyama, K. Ioka and N. Kawanaka, *Phys. Rev. D* **83**, 023002 (2011) [arXiv:1009.1141 [astro-ph.HE]].
 - [21] M. Ackermann *et al.* [Fermi-LAT Collaboration], arXiv:1503.02641 [astro-ph.HE].
 - [22] P. A. R. Ade *et al.* [Planck Collaboration], arXiv:1502.01589 [astro-ph.CO].
 - [23] H. B. Jin, Y. L. Wu and Y. F. Zhou, arXiv:1504.04604 [hep-ph]; M. Ibe, S. Matsumoto, S. Shirai and T. T. Yanagida, arXiv:1504.05554 [hep-ph]. K. Hamaguchi, T. Moroi and K. Nakayama, arXiv:1504.05937 [hep-ph]; S. J. Lin, X. J. Bi, P. F. Yin and Z. H. Yu, arXiv:1504.07230 [hep-ph]; C. H. Chen, C. W. Chiang and T. Nomura, arXiv:1504.07848 [hep-ph].
 - [24] C. Evoli, D. Gaggero and D. Grasso, arXiv:1504.05175 [astro-ph.HE];
 - [25] K. Kohri and N. Sahu, *Phys. Rev. D* **88**, no. 10, 103001 (2013) [arXiv:1306.5629 [hep-ph]].
 - [26] R. B. Larson, *MNRAS* **200**, 159 (1982).
 - [27] A. Whitworth, A., *MNRAS* **186**, 59 (1979).
 - [28] R. Yamazaki, K. Kohri, A. Bamba, T. Yoshida, T. Tsuribe, and F. Takahara, *MNRAS* **371**, 1975 (2006).
 - [29] C. F. McKee and E. C. Ostriker, *ARA & A* **45**, 565 (2007).
 - [30] T. Sjostrand, S. Mrenna, and P. Skands, *JHEP* **05**, 026 (2006).
 - [31] I. V. Moskalenko and A. W. Strong, *ApJ* **493**, 694 (1998).
 - [32] 2013. 33rd Intern. Cosmic Ray Conf., P., ed., Precision Measurement of the Cosmic Ray Boron-to-Carbon Ratio with AMS [AMS collaboration], ed. P. 33rd Intern. Cosmic Ray Conf. (2013)
 - [33] Y. Genolini, A. Putze, P. Salati and P. D. Serpico, *Astron. Astrophys.* **580**, A9 (2015).
 - [34] E. A. Baltz and J. Edsjo, *Phys. Rev. D* **59**, 023511 (1998).
 - [35] A. Bottino, F. Donato, N. Fornengo, and P. Salati, *Phys. Rev. D* **72**, 083518 (2005).
 - [36] A. M. Atoyan, F. A. Aharonian, and H. J. Volk, *Phys. Rev. D* **52**, 3265 (1995).
 - [37] E. Nezri, M. H. G. Tytgat, and G. Vertongen, arXiv:0901.2556.
 - [38] M. Aguilar *et al.* [AMS Collaboration], *Phys. Rev. Lett.* **113**, 121102 (2014).
 - [39] M. Aguilar *et al.* [AMS Collaboration], *Phys. Rev. Lett.* **110**, 141102 (2013).
 - [40] M. Aguilar *et al.* [AMS Collaboration], *Phys. Rev. Lett.* **113**, 221102 (2014).
 - [41] N. Kawanaka, K. Ioka and M. M. Nojiri, *Astrophys. J.* **710**, 958 (2010) [arXiv:0903.3782 [astro-ph.HE]].
 - [42] T. Kobayashi, Y. Komori, K. Yoshida and J. Nishimura, *Astrophys. J.* **601**, 340 (2004) [astro-ph/0308470].
 - [43] T. Linden and S. Profumo, *Astrophys. J.* **772**, 18 (2013) [arXiv:1304.1791 [astro-ph.HE]].
 - [44] M. Ackermann *et al.*, *Phys. Rev. D* **82**, 092003 (2010), arXiv:1008.5119 [astro-ph.HE]
 - [45] N. Kawanaka, K. Ioka, Y. Ohira and K. Kashiyama, *Astrophys. J.* **729**, 93 (2011) [arXiv:1009.1142 [astro-ph.HE]].
 - [46] Y. Ohira and K. Ioka, *Astrophys. J.* **729**, L13 (2011) arXiv:1011.4405 [astro-ph.HE].
 - [47] Q. Yuan and X. J. Bi, *JCAP* **1503**, no. 03, 033 (2015) [arXiv:1408.2424 [astro-ph.HE]].
 - [48] M. Kachelriess, A. Neronov and D. V. Semikoz, arXiv:1504.06472 [astro-ph.HE].